Int J Adv Manuf Technol (2011) 52:477–485
DOI 10.1007/s00170-010-2740-1

ORIGINAL ARTICLE

# Cutting performance of cemented-carbides-based self-lubricated tool embedded with different solid lubricants

**Song Wenlong · Deng Jianxin · Wu Ze · Zhang Hui · Yan Pei · Zhao Jun · Ai Xing**

Received: 21 December 2009 / Accepted: 16 May 2010 / Published online: 29 June 2010


**Abstract** Four micro-holes were made using micro-EDM on rake face of the cemented carbide (WC/TiC/Co) tools. $MoS_2$, $CaF_2$, and graphite solid lubricants were respectively embedded into the four micro-holes to form self-lubricated tools (SLT-1, SLT-2, and SLT-3). Dry machining tests on hardened steel were carried out with these self-lubricated tools and conventional tools (SLT-4). The cutting forces, average friction coefficient between tool and chip, and tool wear were measured and compared. It was shown that the cutting forces and tool wear of self-lubricated tools were clearly reduced compared with those of the SLT-4 conventional tool. The SLT-1 self-lubricated tool embedded with $MoS_2$ just exhibited lower friction coefficient between tool and chip in cutting speed of less than 100 m/min; the SLT-2 self-lubricated tool embedded with $CaF_2$ possessed lower friction coefficient in cutting speed of more than 100 m/min; and the SLT-3 self-lubricated tool embedded with graphite accomplished good lubricating behaviors steadily under the test conditions. It is indicated that cemented carbide inserts with four micro-holes on rake face embedded with appropriate solid lubricants on rake face is an effective way to reduce cutting forces and rake wear.

**Keywords** Dry machining · Self-lubricated tool · Cutting performance · Solid lubricants

S. Wenlong (✉) · D. Jianxin · W. Ze · Z. Hui · Y. Pei · Z. Jun · A. Xing
Department of Mechanical Engineering, Shandong University, Jinan 250061, China
e-mail: wlsong@mail.sdu.edu.cn

## 1 Introduction

Dry machining (without the use of cutting fluid) is an important objective in the industry to reduce environmental pollution and production costs. The advantages of dry machining include [1, 2]: no pollution of the atmosphere or water; no residue on the swarf which will be reflected in reduced disposal and cleaning costs, no danger to health, being non-injurious to skin and allergy free. Dry machining is becoming more and more popular around the world.

In dry machining, there will be more friction and adhesion between the tool and the workpiece since they will be subjected to higher temperature. This will result in increasing tool wear and hence reduction in tool life [3]. It was thought that a reduction in all these problems could be achieved using advanced cutting tool materials to reduce the heat generation by lowering the friction coefficient. For dry machining applications, the cutting tool can be designed in different ways, such as changing tool materials, tool geometries, cutting conditions, workpiece composition, or application of coating tools [4–8]. One of the more promising ways is to develop self-lubricated tools by forming an in situ tribological film with low friction between the work material and tool during the machining processes [9–16].

$MoS_2$, graphite, and $CaF_2$ are all widely used solid lubricants with lamellar structure. The mechanism of effective lubricating performance for these solid lubricants are due to good adhesion to the opposing material and easy shearing along the basal plane of the lamellar structure [17]. The $MoS_2$ and $MoS_2$/metal composite coatings have been successfully applied to dry machining [4–6, 18–21]. However, $MoS_2$ is sensitive to high temperature and begins to be oxidized to $MoO_3$ when

**Table 1** Properties of the cemented carbide tool materials

| Composition (wt%) | Density ($g/cm^3$) | Hardness (GPa) | Flexural strength (MPa) | Thermal conductivity (W/(mK)) | Thermal expansion coefficient ($10^{-6}$/k) |
|---|---|---|---|---|---|
| WC+14%TiC+6%Co | 11.5 | 15.5 | 1130.0 | 33.47 | 6.21 |

**Table 2** Properties of the solid lubricants

| Composition (wt%) | Density ($g/cm^3$) | Size (um) | Melting temperature (°C) | Thermal conductivity (W/(mK)) | Thermal expansion coefficient ($10^{-6}$/k) |
|---|---|---|---|---|---|
| $MoS_2$ | 4.6 | 20 | 1,185 | 0.16 | 10.7 |
| $CaF_2$ | 3.18 | 35 | 1,360 | 9.17 | 18.38 |
| graphite | 2.25 | 20 | 3,527 | 120 | 5.0 |

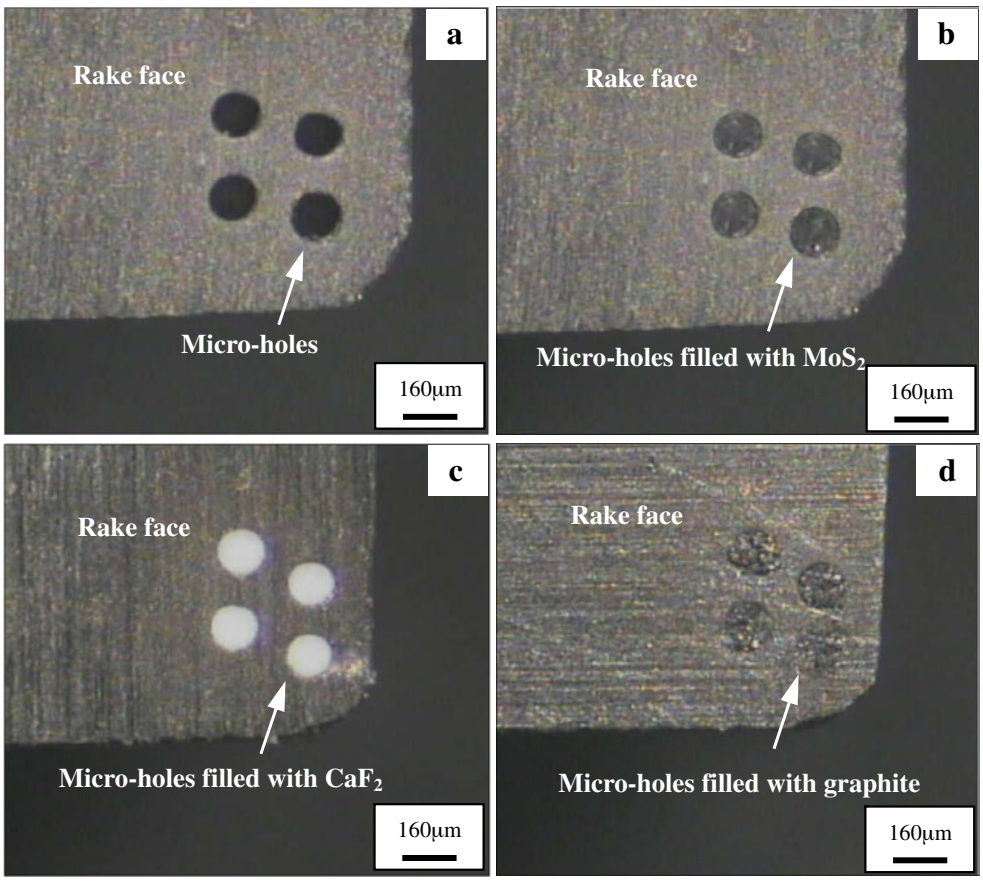


**Fig. 1** Micro-holes in the rake face of the carbide tool filled **a** without solid lubricants, **b** with $MoS_2$ (SLT-1), **c** with $CaF_2$ (SLT-2), **d** with graphite (SLT-3)

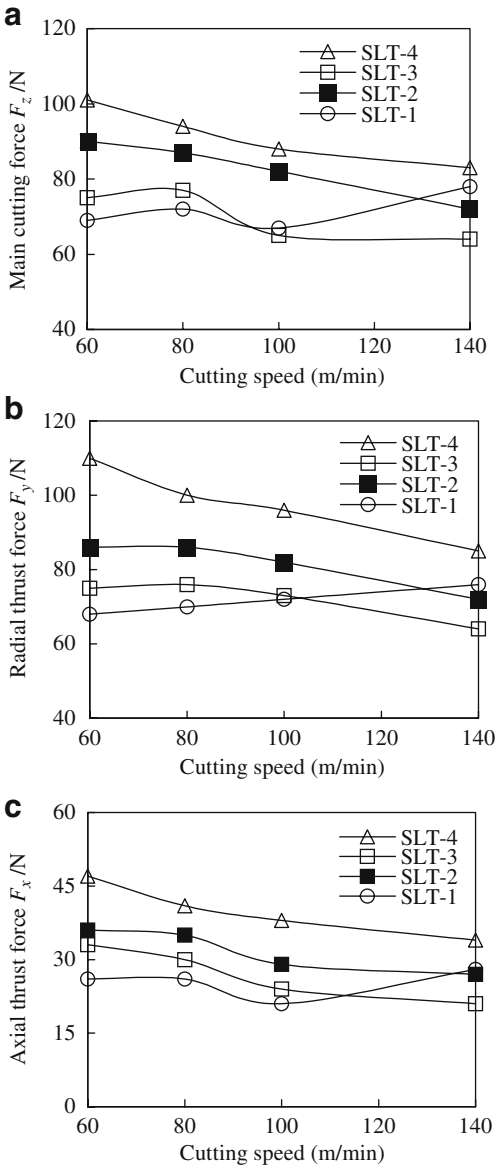


**Fig. 2** Effect of cutting speed on the cutting forces of self-lubricated tools in dry cutting of hardened steel **a** main cutting force $F_z$, **b** radial thrust force $F_y$, and **c** axial thrust force $F_x$ ($a_p$=0.2 mm, feed rates $f$= 0.1 mm/r, cutting time 10 min)

temperature is more than 450°C, causing an increase in friction and a decrease in lifetime. For these reasons, $MoS_2$ and $MoS_2$/metal composite coatings are mainly limited to low-speed continuous cutting or intermittent cutting such as drilling and forming; the friction coefficient of $CaF_2$ solid lubricant is about 0.4 when working temperature is less than 400°C, and the friction coefficient gradually goes down as working temperature increases. The hot-pressed $Al_2O_3$/TiC ceramic tool with the additions of $CaF_2$ solid lubricants shows good self-lubrication especially in higher speed cutting due to higher cutting

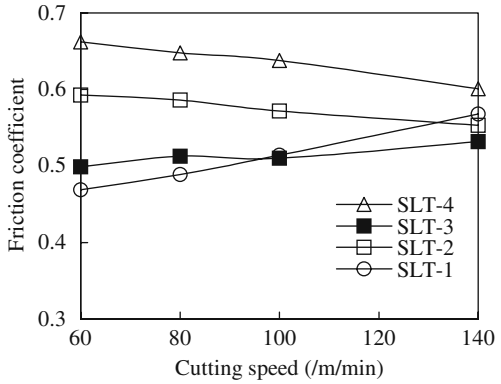


**Fig. 3** Friction coefficient of tools (SLT-1, -2, and -3) in dry cutting of hardened steel ($a_p$=0.2 mm, feed rates $f$=0.1 mm/r, cutting time 10 min)

temperature [9]; graphite is usually used for solid lubricating additives in cutting fluid to reduce the cutting temperature and tool wear [17], which could keep a good lubricating effect in a wide temperature range.

In this study, four micro-holes were made using micro-EDM on the rake face of cemented carbide (WC/TiC/Co) tools. $MoS_2$, $CaF_2$, graphite solid lubricants are respectively filled into the micro-holes to form self-lubricated tools. Continuous machining tests on 45# quenched steel were carried out without cutting fluid. The cutting forces, average friction coefficient at the tool–chip interface and tool wear were measured. The cutting performance of the self-lubricated tools embedded with different solid lubricants was paid to particular attention.

## 2 Experimental procedures

### 2.1 Machining of micro-holes on the cemented carbide inserts

Cemented carbide (WC/TiC/Co) was selected as cutting tool material for this study. Composition, physical, and mechanical properties of this tool material are listed in Table 1. Four micro-holes processed by micro-EDM were fabricated in the proper position at the tool–chip interface of rake face. The diameter of the micro-hole is about 150 μm, and the depth is about 300 μm. Solid lubricants were then filled into the micro-holes so as to form self-lubricated tools. Properties of solid lubricants ($MoS_2$, $CaF_2$, and graphite) are listed in Table 2. Figure 1 shows the four micro-holes on rake face of the cemented carbide insert embedded without and with solid lubricants ($MoS_2$, $CaF_2$, and graphite). The self-lubricated tool with four micro-

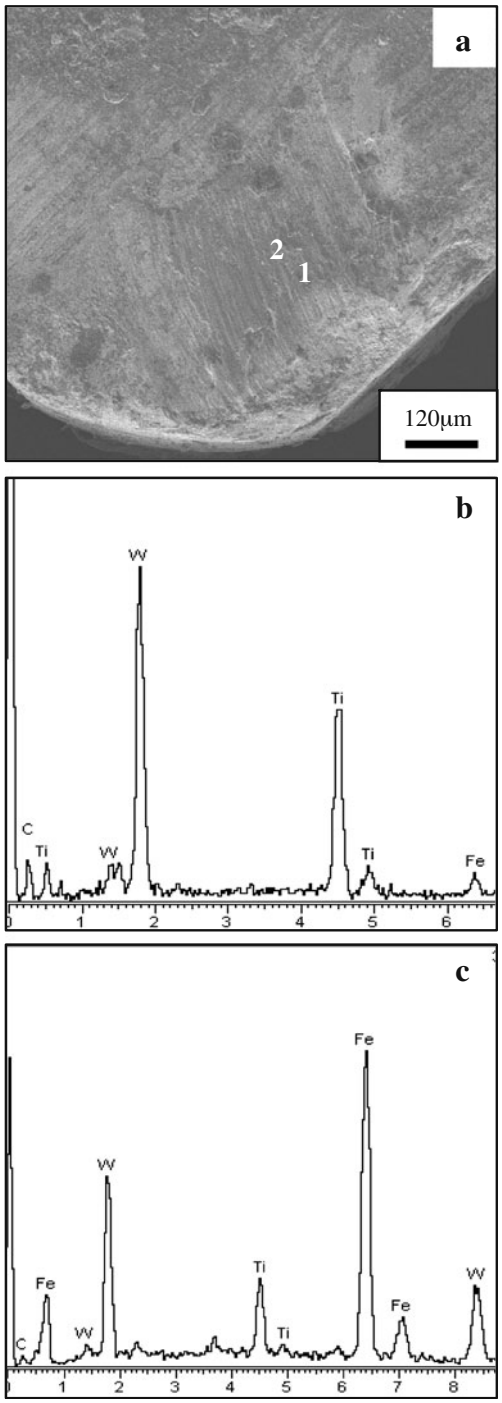


**Fig. 4** SEM micrograph of the worn rake face of SLT-4 tool after 10 min dry cutting of hardened steel at speed of 100 m/min, feed rate of 0.1 mm/r and depth of 0.2 mm **a** SEM micrograph of the worn rake face, **b** EDX composition analysis in selected area point 1 on the wear track, **c** EDX composition analysis in point 2

holes on its rake face filled with $MoS_2$ is named SLT-1, the one with four micro-holes on its rake face filled with $CaF_2$ is named SLT-2, and the one with four micro-holes filled with graphite is named SLT-3.

### 2.2 Cutting tests

Cutting tests were carried out on a CA6140 lathe equipped with a commercial tool holder having the following geometry: rake angle $\gamma_o$=−8°, clearance angle $\alpha_o$=5°, inclination angle $\lambda_s$=5°, side cutting edge angle $k_r$=45°. Cutting tools are used with the SLT-1, SLT-2, SLT-3 self-lubricated tools and conventional tool SLT-4 for comparison. The geometry of the inserts was of ISO SNGN150608. The workpiece materials used were 45# hardened steel (Chinese standard GB99-88) with a hardness of HRC35-40. No cutting fluid was used in the machining processes. All tests were carried out with the following parameters: cut depth $a_p$=0.2 mm, feed rate $f$= 0.1 mm/r, cutting speed $\nu$=60–140 m/min, cutting time= 10 min.

Tool flank wear was measured using a ×20 optional microscope system linked via transducers to a digital readout. Cutting forces were obtained with a KISTLER piezoelectric quartz dynamometer (type 9275A) linked via change amplifiers to a chart recorder. Three experiments were carried out for each test. The worn rake regions of the cutting tools were examined using scanning electron microscope (SEM).

## 3 Results and discussion

### 3.1 Cutting forces

Figure 2 illustrates the main cutting force $F_z$, radial thrust force $F_y$ and axial thrust force $F_x$ as a function of cutting speed with SLT-1, -2, -3, and -4 tools in dry cutting of hardened steel. From this figure, it was found that the cutting force components were clearly reduced with the self-lubricated tools compared with the conventional tool. Meanwhile, it was obvious that cutting speed had a profound effect on the cutting forces. The three cutting force components of the SLT-1 tool embedded with $MoS_2$ solid lubricants are smaller than the other tools in cutting speed of less than 100 m/min. When cutting speed is more than 100 m/min, there is no obvious advantages in reducing cutting forces compared with the other self-lubricated tools; the cutting force variation trend of the SLT-2 self-lubricated tool embedded with $CaF_2$ is different from that of the SLT-1 tool. The cutting forces of SLT-2 tool are obviously reduced in cutting speed of above 100 m/min, while there is no much reduce in cutting forces in comparison with the other self-lubricated tools within cutting speed of below 100 m/min; the SLT-3 tool embedded with graphite solid lubricants exhibits steady cutting performance without sensitivity to cutting speed and cutting temperature during cutting processes.

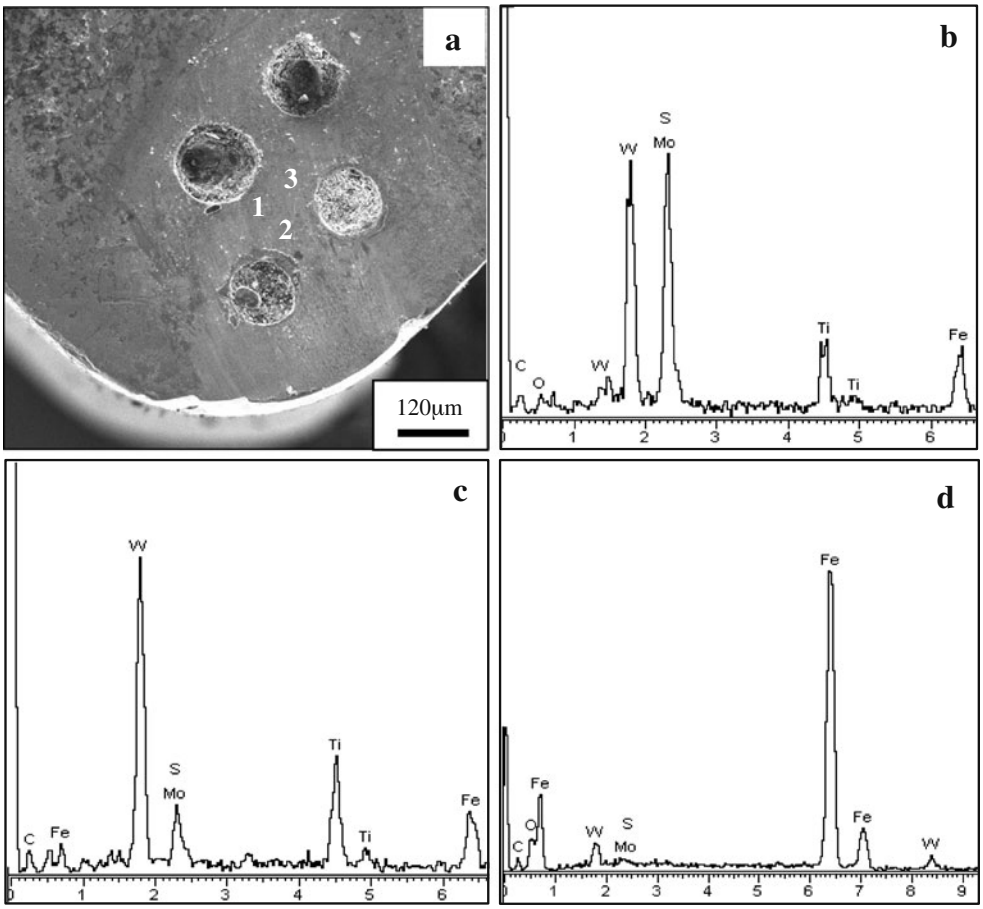


**Fig. 5** SEM and EDX of the worn rake face of SLT-1 tool after 10 min dry cutting of hardened steel at speed of 100 m/min, feed rate of 0.1 mm/r and depth of 0.2 mm **a** SEM micrograph of the worn rake face, **b** EDX composition analysis in selected area point 1 on the wear track, **c** EDX composition analysis in point 2, **d** EDX composition analysis in point 3

### 3.2 Friction coefficient at the tool–chip interface

The average friction coefficient at the tool–chip interface could be calculated based on the following formula [22]:

$$\mu = \tan(\beta) = \tan\left(\gamma_o + \arctan\left(F_y/F_z\right)\right) \quad (1)$$

Where $\beta$ is the friction angle, $\gamma_o$ is the rake angle, $F_y$ is radial thrust force, $F_z$ is the main cutting force.

Figure 3 illustrates the average friction coefficient between tool and chip as a function of cutting speed in dry machining of hardened steel. It can be seen that the average friction coefficients between tool and chip of SLT-1, -2, and -3 tools were greatly reduced compared with that of the conventional tool under the same test conditions. Cutting speed was found to have obvious effect on the average friction coefficient at the tool–chip interface. The SLT-1 tool embedded with $MoS_2$ solid lubricants in the rake face showed lower friction coefficient than the other tools in cutting speed of below 100 m/min. The SLT-2 tool embedded with $CaF_2$ just possessed advantages in reducing friction coefficient in cutting speed of above 100 m/min. The SLT-3 tool embedded with graphite solid lubricants exhibited low friction coefficient without great variation with cutting speed.

### 3.3 Wear patterns at the rake face

Figure 4 shows the SEM micrograph of the worn rake face of SLT-4 tool after 10 min dry cutting of hardened steel at speed of 100 m/min, feed rate of 0.1 mm/r and cut depth of 0.2 mm. Serious surface damage in the form of abrasive and adhesive wears can be observed on the rake face shown in Fig. 4a. The EDX surface chemical composition analysis in selected area point 1 and 2 on the wear track are shown in Fig. 4b and c, respectively. W and Ti elements of tool material were identified in point 1 and 2; while Fe element was observed at point 2 and 3 on the worn surface. It exhibited that the rake face was covered by the transferred workpiece material due to intensive adhesion and plastic flow. The repeated adhering and friction of the workpiece to the rake face may lead to tool wears because of high pressure and cutting temperature.

The SEM micrograph of the wear track at the rake face of SLT-1 self-lubricated tool after 10-min cutting at

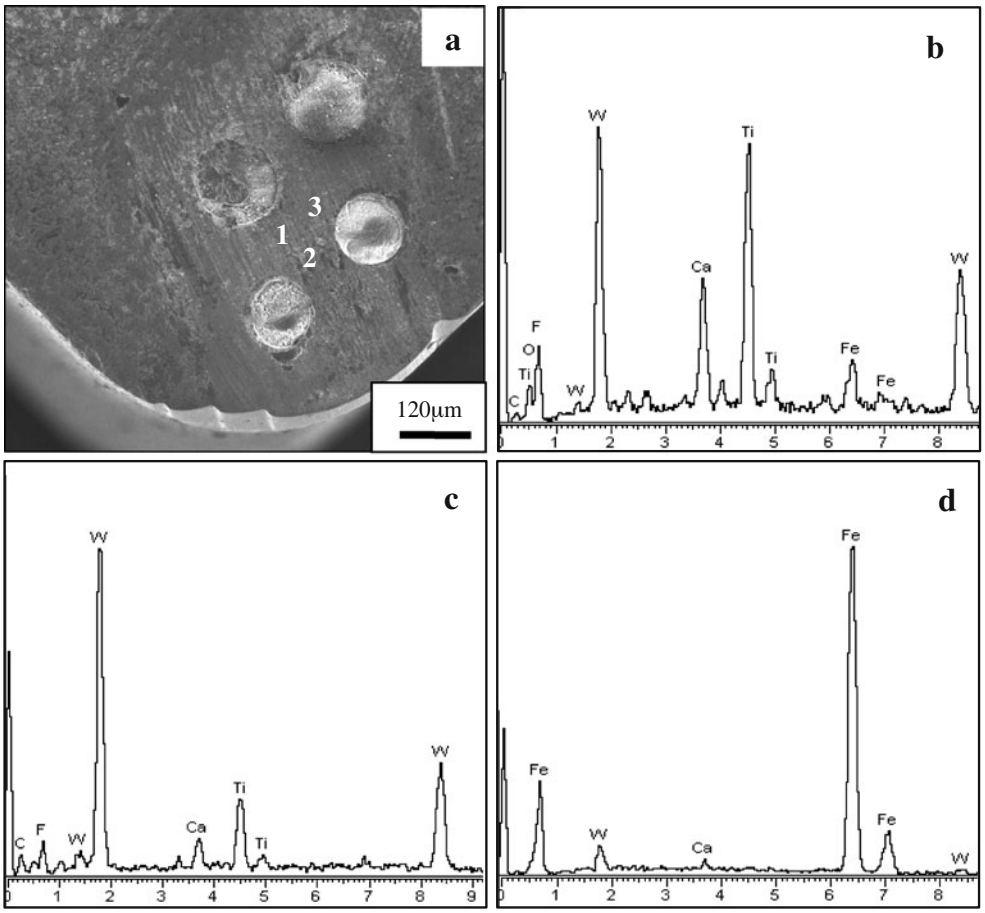


**Fig. 6** SEM and EDX of the worn rake face of SLT-2 tool after 10 min dry cutting of hardened steel at speed of 100 m/min, feed rate of 0.1 mm/r, and depth of 0.2 mm **a** SEM micrograph of the worn rake face, **b** EDX composition analysis in selected area point 1 on the wear track, **c** EDX composition analysis in point 2, **d** EDX composition analysis in point 3

speed of 100 m/min is shown in Fig. 5a. It is shown that the SLT-1 self-lubricated tool did not experience as serious wear as that of SLT-4 conventional tool because of lower cutting forces and friction coefficient at the tool–chip interface. The Fig. 5b and c revealed that the S and Mo elements were identified in worn area. These S and Mo elements maybe transferred from the micro-holes and smeared on the rake face. It seemed that a thin lubricating film was formed on the wear track. Figure 5b, c, and d are the EDX surface chemical composition analysis on the wear track (point 1, 2 and 3). They indicate that the thin lubricating film formed on the wear track was unevenly smeared on the tool face due to high pressure and chip friction.

The SEM and EDX element distribution analysis of self-lubricated tool with four micro-holes embedded with solid lubricants on the rake face of SLT-2 and -3 tools are shown in Figs. 6 and 7. They indicate that the solid lubricants ($CaF_2$ and graphite) could be smeared on rake face from the micro-holes of self-lubricated tools; and a thin uneven lubricating film could form on the wear track during machining processed.

## 4 Discussion

The three cutting force components on the tool–chip interface under elasticity loaded conditions in an elasticity contact can be simplified as [22–27]:

$$F_z = a_w l_f \tau_c \left( \sin\gamma_o - \frac{\cos\gamma_o}{tg\beta} \right) \tag{2}$$

$$F_x = a_w l_f \tau_c \left( \cos\gamma_o - \frac{\sin\gamma_o}{tg\beta} \right) \cos(\psi_r + \psi_\lambda) \tag{3}$$

$$F_y = a_w l_f \tau_c \left( \cos\gamma_o - \frac{\sin\gamma_o}{tg\beta} \right) \sin(\psi_r + \psi_\lambda) \tag{4}$$

Where $\tau_c$ is average shear stress on the rake face of tool, which may be a lubricant film, $l_f$ is contact length between the tool and chip, $\alpha_w$ is cut width, $\psi_\lambda$ is chip flow angle, $\psi_r$ is approach angle.

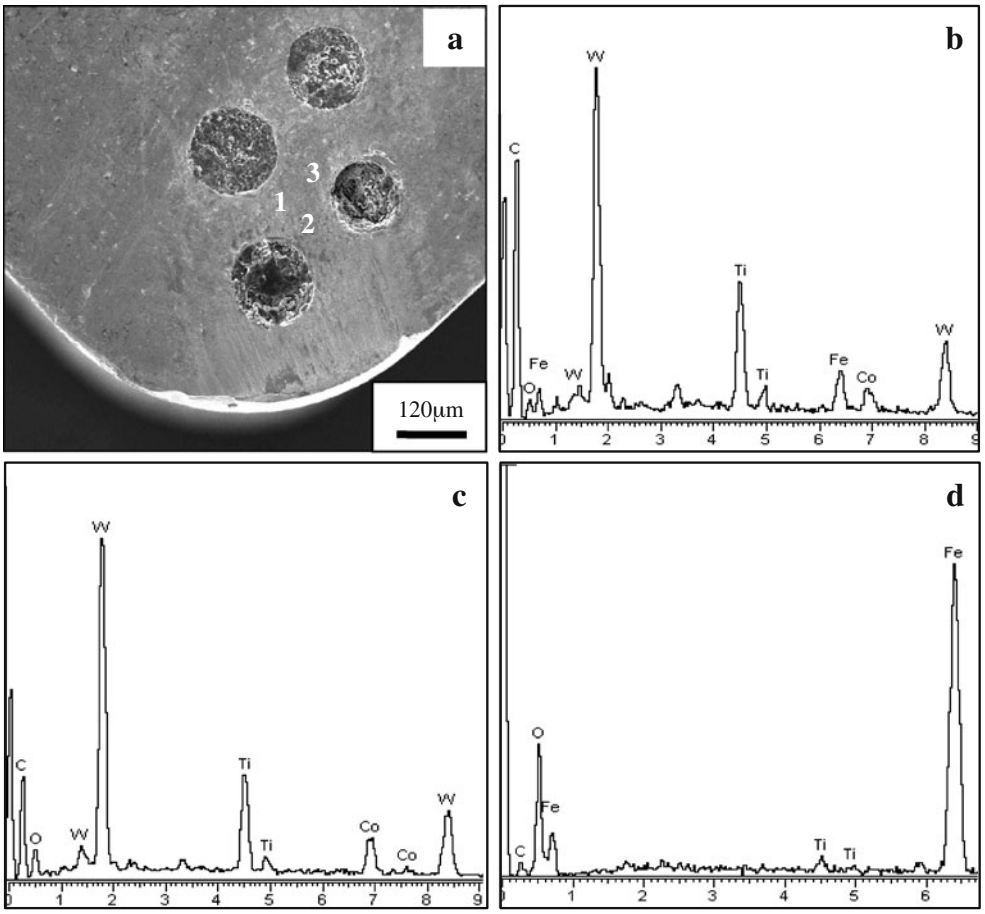


**Fig. 7** SEM and EDX of the worn rake face of SLT-3 tool after 10 min dry cutting of hardened steel at speed of 100 m/min, feed rate of 0.1 mm/r and depth of 0.2 mm **a** SEM micrograph of the worn rake face, **b** EDX composition analysis in selected area point 1 on the wear track, **c** EDX composition analysis in point 2, **d** EDX composition analysis in point 3

The above parameters including cut width $\alpha_w$, rake angle $\gamma_o$, and approach angle $\psi_r$, have been given in practical cutting. The chip flow angle $\psi_\lambda$ remains basically unchanged under the same processing conditions.

For a given contact geometry Eqs. 2, 3, and 4 shows that the cutting forces vary linearly with critical shear stress $\tau_c$ and contact length $l_f$ between the chip and tool. When there is a lubricant film on the wear surface, the matrix endures the load, and friction occurs on the lubricant film [20, 21]. As the lubricant film on the wear surface has a much smaller critical shear stress than the insert substrate, and thus results in reduce of cutting forces according to Eqs. 2, 3 and 4. This means that the lubricating film on the tool rake face can act as lubricants, and self-lubrication can be accomplished. The figures (Figs. 6 and 7) above had proved that there were solid lubricants on the tool face, which were released and smeared from the micro-holes of the self-lubricated tools.

When there is a reduction of contact area $l_f$ between the chip and tool, there will also be produce a linearly reduction of cutting forces according to Eqs. 2, 3, and 4. Once the micro-holes are fabricated at the tool–chip interface of the tool face, the contact area $l_f$ between chip and tool will decrease, and the cutting forces will be reduced compared with those of the conventional tools if the micro-holes do not seriously degrade the mechanical properties of tool substrate. Then the friction coefficient between tool and chip will decrease.

Therefore, there are two factors that affect the cutting performance of the self-lubricated tools. One is a reduction in contact length $l_f$ between chip and tool, the other is owing to forming a lubricating film with low shear stress, which resulted in reduced average shear stress $\tau_c$.

The different cutting performances of self-lubricated tools embedded with various solid lubricants were considered to be different physical properties of solid lubricants. The SLT-1 self-lubricated tool embedded with $MoS_2$ showed better self-lubricating behaviors with lower cutting forces and friction coefficient in cutting speed of less than 100 m/min, but it exhibited worse self-lubricating effect in cutting speed of more than 100 m/min. This is because that $MoS_2$ is sensitive to high cutting speed [28], which leads to high cutting temperature. It begins to be oxidized to $MoO_3$ when working temperature is more than 450°C, causing an increase in friction and a decrease in lifetime; The cutting forces of SLT-2 self-lubricated tool embedded with $CaF_2$ are smaller just in cutting speed of more than 100 m/min because $CaF_2$ material is sensitive to lower temperature. The friction coefficient of $CaF_2$ solid lubricant is about 0.4 when working temperature is less than 400°C, and the

friction coefficient gradually decreases as working temperature increases from 400°C; the SLT-3 self-lubricated tool embedded with graphite could accomplish self-lubricating behaviors better under the test conditions due to no obvious sensitivity to cutting speed and temperature.

Further work will include the following: the extension of the micro-holes in terms of changing number of holes, depth of holes, array of holes, etc. needs a solid justification; what is the cutting performance, if no more solid lubricants can be available after a long period cutting; what is the effect of hole-introduced stress concentration on the tool cutting performance after some time machining operation.

## 5 Conclusions

Four micro-holes were made using micro-EDM in the rake face of the cemented carbide (WC/TiC/Co) tools. $MoS_2$, $CaF_2$ and graphite solid lubricants were respectively embedded into the four micro-holes to form self-lubricated tools (SLT-1, -2, and -3). Dry machining tests on hardened steel were carried out with these self-lubricated tools and the conventional tool SLT-4. The following conclusions can be obtained:

(a) In this experimental condition, the self-lubricated tools with four micro-holes on rake face embedded with solid lubricants possessed better cutting properties. The cutting forces and average friction coefficient between tool and chip of self-lubricated tools were reduced compared with those of SLT-4 conventional tool, which resulted in reduced rake wear.

(b) The primary mechanism of the cutting force-decreasing effect of self-lubricated tools was put forward: one was the reduction of contact length between chip and tool; the other was the formation of a self-lubricating film between the sliding couple, which was released from the micro-holes and smeared on tool face.

(c) In agreement with physical properties of solid lubricants, the self-lubricating tools embedded with different solid lubricants possessed different lubricating behaviors due to sensitivity to cutting speed (cutting temperature). The SLT-1 self-lubricated tool just exhibited good self-lubricating effect in cutting speed of below 100 m/min, the forces of SLT-2 self-lubricated tool were reduced much just in cutting speed of above 100 m/min, and the SLT-3 self-lubricated tool possessed steady lubricating behaviors under the test conditions.

**Acknowledgments** This work was supported by "Taishan Scholar Program Foundation of Shandong", "Outstanding Young Scholar Science Foundation of Shandong (JQ200917)" and "National High Technology Research and Development Program (2009AA044303)", and 973 Program (2009CB724402).

## References

1. Klocke F, Eisenblatter G (1997) Dry cutting. Ann CIRP 46 (2):519–526
2. Sreejith PS, Ngoi BKA (2000) Dry machining: machining of the future. J Mater Process Technol 101:287–291
3. Deng JX, Ai X, Feng YH (2002) Wear lubrication and matching of cutting tools with the work piece materials. Chinese J Mech Eng 38(4):40–45
4. Renevier NM, Hamphire J, Fox VC (2001) Advantages of using self-lubricating, hard, wear-resistant $MoS_2$-based coatings. Surf Coat Tech 142–144:67–77
5. Renevier NM, Oosterling H, König U, Dautzenberg H, Kim BJ, Geppert L, Koopmans FGM, Leopold J (2003) Performance and limitation of hybrid PECVD (hard coating)-PVD magnetron sputtering ($MoS_2$/Ti composite) coated inserts tested for dry high speed milling of steel and grey cast iron. Surf Coat Tech 163–164:659–667
6. Renevier NM, Oosterling H (2003) Performance and limitations of $MoS_2$/Ti composite coated inserts. Surf Coat Tech 172(1):13–23
7. Deng JX, Liu JX, Zhao JL, Song WL (2008) Wear mechanisms of PVD ZrN coated tools in machining. J Refract Met Hard Mater 26:164–172
8. Deng JX, Liu JX, Zhao JL, Song WL, Niu M (2008) Friction and wear behaviors of the PVD ZrN coated carbide in sliding wear tests and in machining processes. Wear 264:298–307
9. Rivero A, Aramendi G, Herranz S, de Lacalle LNL (2006) An experimental investigation of the effect of coatings and cutting parameters on the dry drilling performance of aluminium alloys. Int J Adv Manuf Technol 28:1–11
10. Dos Santos JABO, Sales WF, Santos SC, Machado AR, da Silva MB, Bonney J, Ezugwu EO (2007) Tribological evaluation of TiN and TiAlN coated PM-HSS gear cutter when machining 19MnCr5 steel. Int J Adv Manuf Technol 31:629–637
11. Tsao CC (2007) An experiment study of hard coating and cutting fluid effect in milling aluminum alloy. Int J Adv Manuf Technol 32:885–891
12. Abdel-Aal HA, Nouari M, El Mansori M, Ginting A (2008) Conceptual tribo-energetic analysis of cutting tool protective coating delamination in dry cutting of hard-to-cut aero engine alloys. Int J Adv Manuf Technol 36:213–225
13. Deng JX, Cao TK, Yang XF (2006) Self lubrication of sintered ceramic tools with $CaF_2$ additions in dry cutting. Int J Mach Tools Manuf 46(9):957–963
14. Deng JX, Cao TK (2005) Self-lubricating behaviors of $Al_2O_3$/$TiB_2$ ceramic tools in dry high-speed machining of hardened steel. J Eur Ceram Soc 25(7):1073–1079
15. Deng JX, Cao TK, Yang XF (2007) Wear behavior and self tribofilm formation of hot-pressed $Al_2O_3$/TiC/$CaF_2$ ceramic composites sliding against cemented carbide. Ceram Int 33:213–220
16. Aizawa T, Mitsuo A, Yamamoto S, Sumitomo T, Muraishi S (2005) Self-lubrication mechanism via the in situ formed lubricious oxide tribofilm. Wear 259:708–718
17. Senda T, Yamamoto Y, Ochi Y (1993) Friction and wear test of titanium boride ceramics at elevated temperatures. J Am Ceram Soc 101(4):461–465
18. Deng JX, Cao TK, Ding ZL (2006) Tribological behaviors of hot-pressed $Al_2O_3$/TiC ceramic composites with the additions of $CaF_2$ solid lubricants. J Eur Ceram Soc 26(8):1317–1323
19. Deng JX, Song WL, Zhang H (2009) Design, fabrication and properties of a self-lubricated tool in dry cutting. Int J Mach Tools Manuf 49:66–72
20. Shi MS (2000) Solid lubricating materials. China Chemical Industry Press, Beijing

21. Deng JX, Song WL, Zhang H, Zhao JL (2008) Performance of PVD $MoS_2$/Zr-coated carbide in cutting processes. Int J Mach Tools Manuf 48:1546–1552
22. Renevier NM, Fox VC, Teer DG, Hampshire J (2000) Performance of low friction $MoS_2$/titanium composite coatings used in forming applications. Mater Design 21:337–343
23. Rigato V, Maggioni G, Patelli A, Renevier NM, Teer DG (2000) Properties of sputter-deposited $MoS_2$/metal composite coatings deposited by closed field unbalanced magnetron sputter ion plating. Surf Coat Tech 131:206–210
24. Chen RY (1993) Metal-cutting principles. China Machine Press, Beijing
25. Nakayama K (1985) Principle of metal cutting. China Machine Press, Beijing
26. Usui E (1982) Mechanical metal processing. China Machine Press, Beijing
27. Liu PD (1991) New development in mechanics of cutting. Dalian Technical University Press, Dalian
28. Wen SZ (1990) Tribological principles. Tsinghua University Press, Beijing